

Supporting Information

X-ray Absorption Spectroscopic Characterization of the Diferric-peroxo Intermediate of Human Deoxyhypusine Hydroxylase in the Presence of its Substrate eIF5a

Andrew J. Jasniewski^a, Lisa M. Engstrom^a, Van V. Vu^a, Myung Hee Park^b, Lawrence Que, Jr.^{a,*}

^a*Department of Chemistry and Center for Metals in Biocatalysis, University of Minnesota, 207 Pleasant St. SE, Minneapolis, MN 55455;*

^b*National Institute of Dental and Craniofacial Research, National Institutes of Health, 9000 Rockville Pike, Bethesda, MD 20892*

Table of Contents

Figure S1. UV-vis of hDOHH-P and hDOHH-P•S	Page 2
Figure S2. Pre-edge analysis of hDOHH-R	Page 3
Figure S3. EXAFS spectrum of hDOHH-R	Page 3
Table S1. EXAFS fit of hDOHH-R	Page 4
Figure S4. Pre-edge analysis of hDOHH-P	Page 5
Figure S5 EXAFS spectrum of hDOHH-P	Page 6
Table S2. EXAFS fit of hDOHH-P	Page 7
Figure S6. Pre-edge analysis of hDOHH-P•S	Page 8
Figure S7 EXAFS spectrum of hDOHH-P•S	Page 8
Table S3. EXAFS fit of hDOHH- P•S	Page 9
Figure S8 Pre-edge analysis of hDOHH-D	Page 10
Figure S9 EXAFS spectrum of hDOHH-D, Fit A	Page 10
Figure S10 EXAFS spectrum of hDOHH-D, Fit B	Page 11
Table S4. EXAFS fit of hDOHH-D, Fit A	Page 11
Table S5. EXAFS fit of hDOHH-D, Fit B	Page 12
Figure S11. Pre-edge analysis of hDOHH-D•S	Page 12
Figure S12 EXAFS spectrum of hDOHH-D•S	Page 13
Table S6. EXAFS fit of hDOHH-D•S	Page 14
Table S7. Pre-edge Component Analysis	Page 14
Table S8. Fe ^{II} model complex distances	Page 15
Table S9. Fe ^{III} model complex distances	Pages 16-17

General EXAFS considerations: In the fit tables of EXAFS data, N refers to the number of scatterers used for a particular shell, R is the distance of the scattering shell, σ^2 is the mean-squared deviation (or Debye-Waller factor), E_0 is the edge shift parameter, and the goodness of fit (GOF) parameters are calculated as $F = \sqrt{\sum k^6 (\chi_{\text{exp}} - \chi_{\text{calc}})^2}$, $F' = \sqrt{\sum k^6 (\chi_{\text{exp}} - \chi_{\text{calc}})^2 / \sum k^6 \chi_{\text{exp}}^2}$. For all fits, the amplitude reduction factor (S_0^2) was set to 0.9.

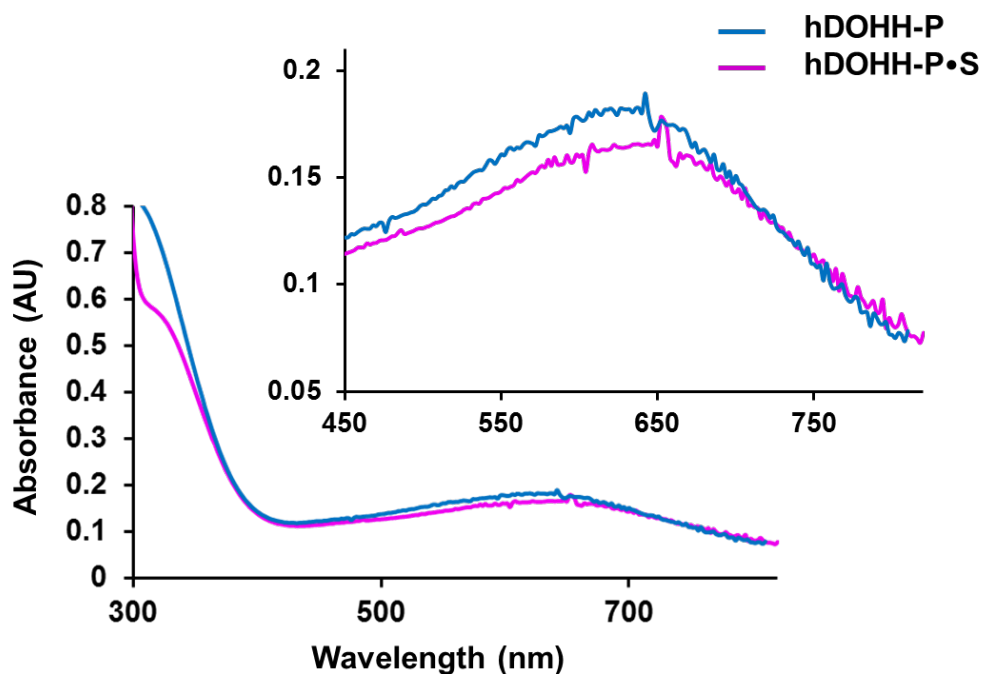


Figure S1. UV-visible absorption spectra of hDOHH-**P** (blue) and hDOHH-**P•S** (purple). Concentration of hDOHH-**P** in both samples is 75 μM with 1.2 eq. of eIF5A(Dhp) added to make the hDOHH- **P•S** sample. Both samples were prepared in 50 mM Tris-HCl, 125 mM NaCl buffer with spectra recorded at 25 °C. Inset: zoom in on the 630 nm LMCT transition.

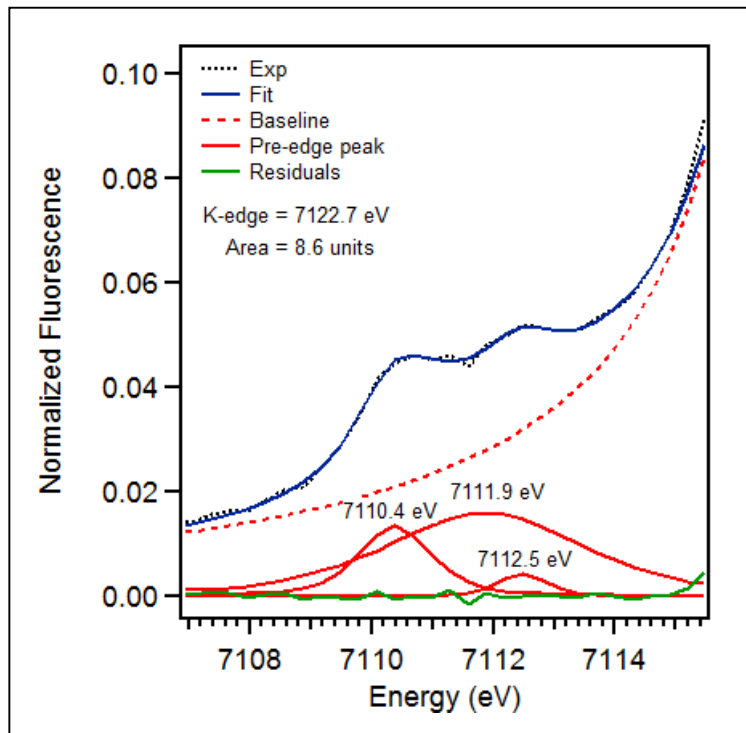


Figure S2. Pre-edge region analysis of hDOHH-R. The experimental data (black dotted), baseline (red dashed), pre-edge peak components (red solid), residuals (green solid) and total fit (blue solid) are shown.

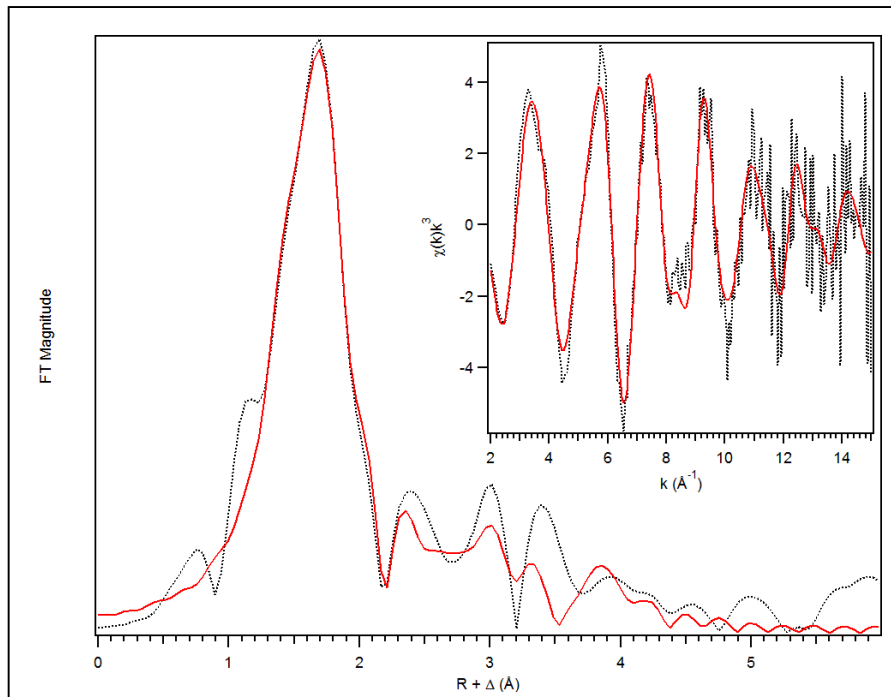


Figure S3. EXAFS spectrum of hDOHH-R. Fit (red solid line) of the unfiltered (black dotted) EXAFS data (inset) and corresponding Fourier transform (Table S1, Fit 12). Data was fit between $k = 2 - 15 \text{ Å}^{-1}$.

Table S1. Fit parameters for the unfiltered EXAFS data of hDOHH-R, between $k = 2 - 15 \text{ \AA}^{-1}$.
 Fit 12 gives the most reasonable fit of the experimental data.

Fit	Fe-N				Fe-O				Fe...Fe				Fe...C				GOF		
	N	R(Å)	$\sigma^2(10^{-3})$	E _o	F	F'													
1	6	2.15	4.71										-5.97	360	509				
2	5	2.15	3.73										-5.59	384	526				
3	4	2.15	2.71										-5.16	433	558				
4	5	2.17	3.01	1	2.05	1.77							-6.97	350	503				
5	4	2.18	2.54	2	2.07	3.25							-7.55	347	500				
6	5	2.17	3.30	1	2.05	2.27				3	3.11	5.41	-6.21	317	478				
7	4	2.18	2.85	2	2.08	3.49				3	3.10	5.49	-6.69	313	475				
8	4	2.17	2.64	2	2.07	3.51	1	3.46	7.04	3	3.09	6.58	-7.28	299	464				
9	5	2.17	3.04	1	2.05	1.88	1	3.47	7.17	3	3.10	6.48	-6.72	304	468				
10	5	2.17	3.19	1	2.05	2.02	1	3.47	7.26	3	3.10	6.56	-6.20	287	453				
										4	4.36	3.61							
11	4	2.18	2.99	2	2.08	3.92	1	3.46	7.02	3	3.09	6.54	-6.70	281	450				
										4	4.35	3.24							
12	4	2.18	2.78	2	2.07	3.39	1	3.47	5.18	3	3.10	6.20	-6.80	272	443				
										3	3.68	4.05							
										3	4.35	2.51							
13	5	2.17	3.15	1	2.05	1.85	1	3.47	5.33	3	3.11	6.13	-6.36	277	446				
										3	3.68	3.79							
										3	4.36	2.88							
14	5	2.17	3.42	1	2.06	2.32				3	3.11	5.39	-5.70	280	449				
										3	4.05	2.01							
										4	4.36	1.81							
15	5	2.17	3.05	1	2.05	1.75	1	3.46	5.07	3	3.69	4.64	-7.01	299	464				
										4	4.35	2.57							
16	5	2.16	3.10	1	2.05	2.07	1	3.47	6.10	3	3.10	6.34	-7.05	300	465				
										3	3.70	4.78							
17	4	2.17	2.72				1	3.48	5.86	3	3.12	5.85	-4.80	354	505				
										3	3.70	3.70							
										4	4.37	2.17							
18	6	2.15	4.71				1	3.48	5.79	3	3.12	5.97	-5.70	286	454				
										3	3.69	3.62							
										4	4.37	2.25							

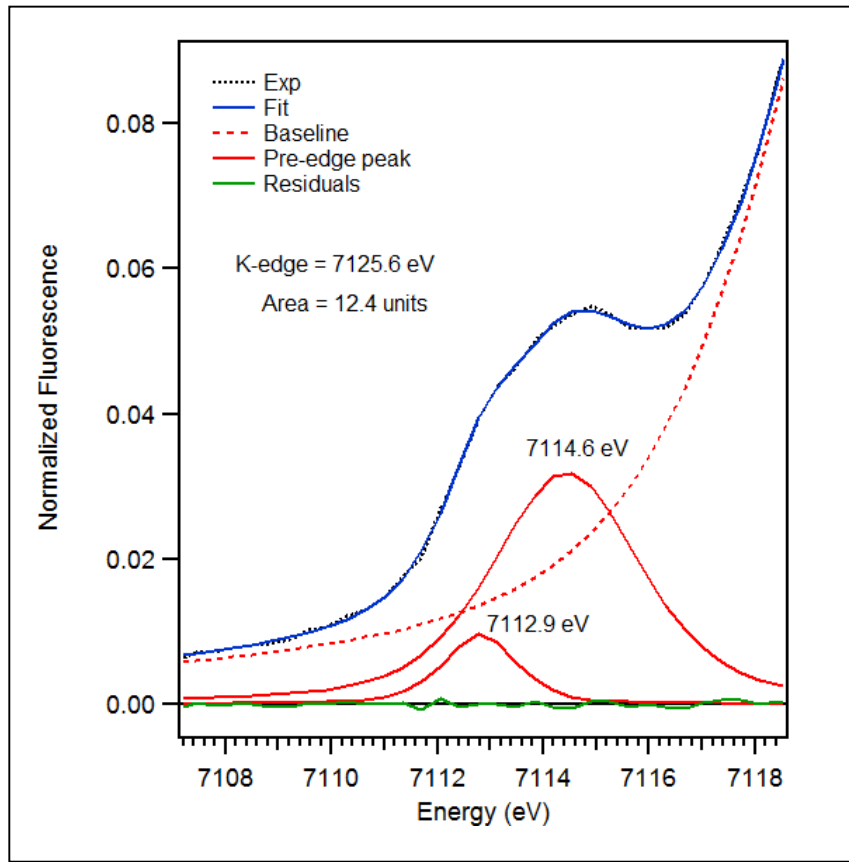


Figure S4. Pre-edge region analysis of hDOHH-**P**. The experimental data (black dotted), baseline (red dashed), pre-edge peak components (red solid), residuals (green solid) and total fit (blue solid) are shown

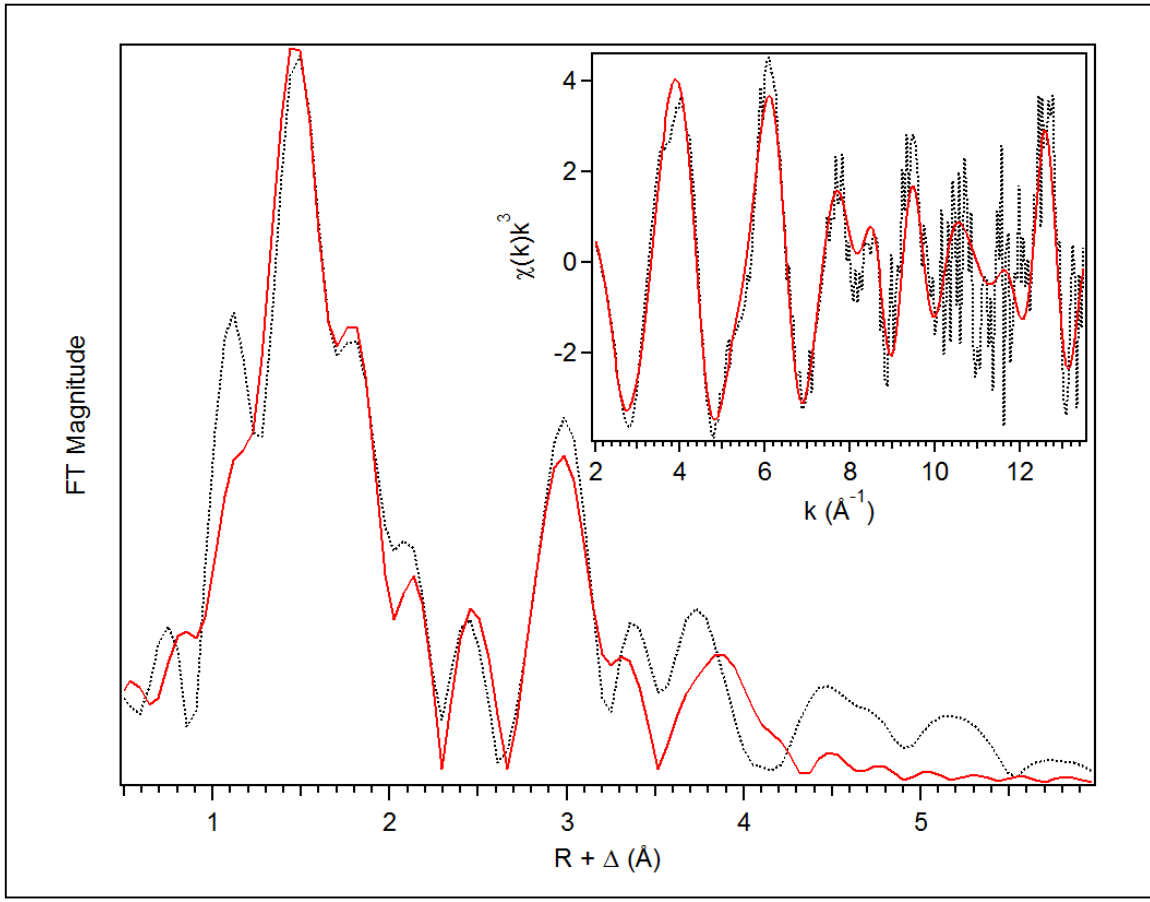


Figure S5. EXAFS spectrum of hDOHH-**P**. Fit (red solid line) of the unfiltered (black dotted) EXAFS data (inset) and corresponding Fourier transform (Table S2, Fit 14). Data was fit between $k = 2 - 13.5 \text{ \AA}^{-1}$.

Table S2. Fit parameters for the unfiltered EXAFS data of hDOHH-P, between $k = 2 - 13.5 \text{ \AA}^{-1}$.
 Fit 14 gives the most reasonable fit of the experimental data.

Fit	Fe-N				Fe-O				Fe \cdots Fe				Fe \cdots C				GOF		
	N	R(Å)	$\sigma^2(10^{-3})$	N	R(Å)	$\sigma^2(10^{-3})$	N	R(Å)	$\sigma^2(10^{-3})$	N	R(Å)	$\sigma^2(10^{-3})$	E _o	F	F'				
1	6	2.08	12.12										0.79	392	637				
2	5	2.08	10.51										1.30	410	652				
3	4	2.09	8.80										2.31	446	680				
4	3	2.11	6.86										3.63	504	723				
5	3	2.13	1.44	1	1.97	-1.40							1.19	331	586				
6	3	2.15	1.33	2	1.98	1.73							-0.21	305	562				
7	4	2.14	3.10	2	1.96	2.04							-0.32	300	558				
8	3	2.15	0.56	2	1.99	0.74							-2.27	297	554				
				1	1.90	4.49													
9	3	2.14	1.46	2	1.97	1.82	1	3.42	3.05				-0.79	233	491				
10	3	2.14	1.36	2	1.97	1.77	1	3.42	3.33	3	4.30	0.08	-0.60	209	465				
11	3	2.14	1.37	2	1.97	1.79	1	3.42	3.30	4	4.30	1.51	-0.51	207	464				
12	3	2.15	0.99	2	1.99	1.63	1	3.41	3.21	4	2.29	1.61	-2.09	198	453				
				1	1.91	6.68							3	3.60	3.31				
13	3	2.14	1.53	2	1.97	1.93	1	3.42	2.03	4	4.30	1.44	-0.78	197	452				
													3						
14	3	2.15	1.95	3	1.98	4.57	1	3.41	1.86	4	4.29	1.55	-1.76	190	444				
													3	3.58	2.93				

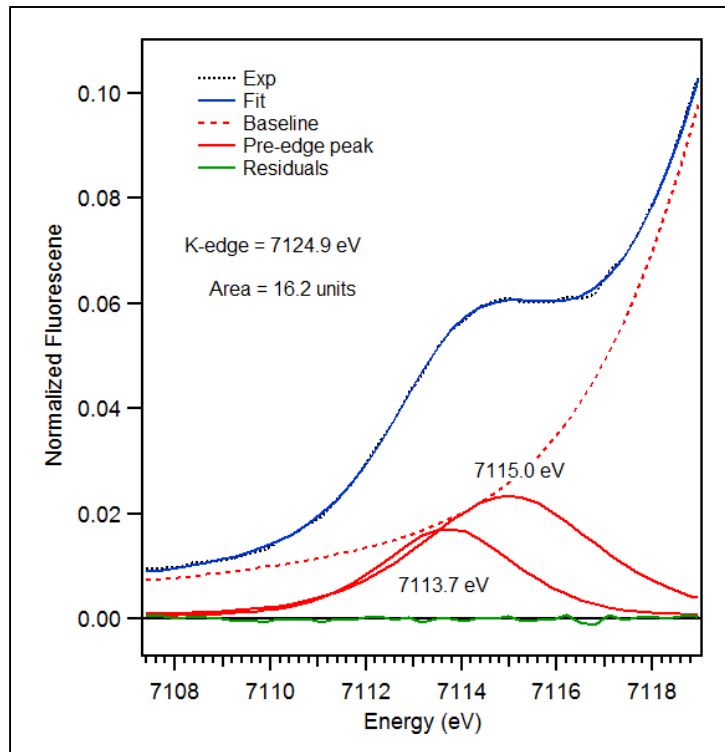


Figure S6. Pre-edge region analysis of hDOHH-**P•S**. The experimental data (black dotted), baseline (red dashed), pre-edge peak components (red solid), residuals (green solid) and total fit (blue solid) are shown

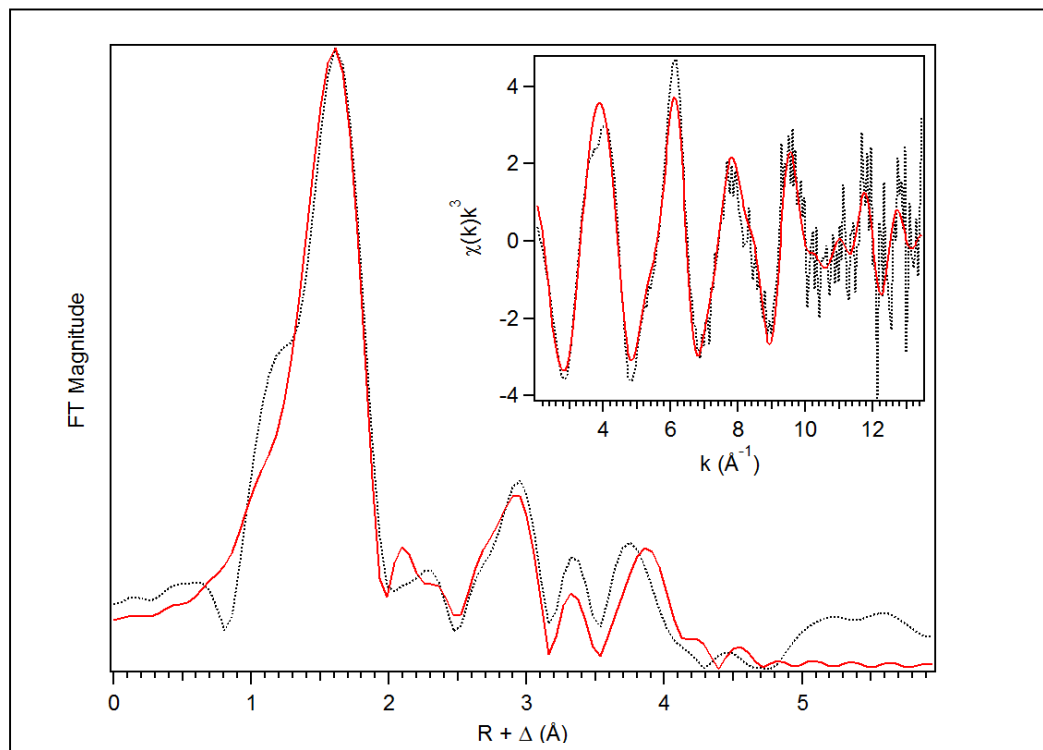


Figure S7. EXAFS spectrum of hDOHH-**P•S**. Fit (red solid line) of the unfiltered (black dotted) EXAFS data (inset) and corresponding Fourier transform (Table S3, Fit 17). Data was fit between $k = 2 - 13.5 \text{ \AA}^{-1}$.

Table S3. Fit parameters for the unfiltered EXAFS data of hDOHH-P•S, between $k = 2 - 13.5 \text{ \AA}^{-1}$. Fit 17 gives the most reasonable fit of the experimental data.

Fit	Fe-N			Fe-O			Fe...Fe			Fe...C			GOF		
	N	R(Å)	$\sigma^2(10^{-3})$	N	R(Å)	$\sigma^2(10^{-3})$	N	R(Å)	$\sigma^2(10^{-3})$	N	R(Å)	$\sigma^2(10^{-3})$	E_o	F	F'
1	6	2.08	9.45										-4.13	228	540
2	5	2.08	7.76										-3.40	223	553
3	4	2.09	6.06										-2.86	233	546
4	3	2.09	4.29										-2.25	268	585
5	3	2.12	4.15	1	2.00	1.90							-2.51	212	521
6	3	2.10	12.28	2	2.05	5.41							-3.18	208	516
7	4	2.11	6.48	1	1.99	4.77							-3.34	210	518
8	4	2.12	5.70	1	1.99	3.17	1	3.07	7.49				-2.67	169	465
9	4	2.12	5.69	1	1.99	3.00				3	3.10	3.26	-2.67	170	465
10	4	2.11	5.48	1	1.98	3.44	1	3.07	7.44	4	4.30	1.31	-2.65	143	427
11	4	2.11	5.86	1	1.99	3.61	1	3.08	8.0	4	4.30	1.42	-3.00	140	423
										2	3.41	4.02			
12	4	2.10	5.94	1	1.97	5.86				4	4.29	1.30	-4.46	172	469
										2	3.43	1.42			
13	4	2.11	5.50	1	1.97	4.24				4	4.30	1.15	-3.62	134	414
										2	3.43	3.15			
										3	3.09	3.71			
14	4	2.11	5.43	1	1.97	4.05				3	3.09	3.28	-3.62	146	432
										4	4.30	1.16			
15	4	2.10	5.67	1	1.97	4.99	1	3.43	7.95	4	4.29	0.98	-4.44	164	458
16	4	2.1	5.24	1	1.97	3.80	1	3.43	10.99	3	3.09	3.97	-3.87	135	414
										4	4.29	3.99			
17	4	2.11	5.61	1	1.98	4.47	1	3.41	5.44	3	3.09	6.50	-3.90	132	411
										3	3.56	3.51			
										4	4.30	1.72			
18	4	2.11	5.75	1	1.98	4.52	1	3.41	5.61	3	3.61	3.20	-4.00	38	421
							1	3.07	11.32	4	4.29	1.92			
19	4	2.10	6.32	2	1.98	10.78	1	3.48	13.37	2	3.38	1.82	-5.34	140	424
							1	3.07	10.03	4	4.28	1.32			
20	5	2.09	7.05	1	1.94	8.36	1	3.07	8.68	3	3.41	5.49	-4.94	148	435
										4	4.28	1.02			
21	4	2.09	5.95	2	1.96	11.61	1	3.40	4.58	3	3.08	7.63	-5.84	134	414
										3	3.59	2.50			
										4	4.28	2.02			
22	4	2.10	5.83	1.5	1.97	8.81	1	3.40	4.99	3	3.08	7.24	-5.14	132	411
										3	3.59	3.17			
										4	4.29	1.66			
23	4.5	2.09	6.41	1.5	1.95	10.26	1	3.41	4.71	3	3.08	7.13	-5.40	135	416
										3	3.60	2.45			
										4	4.29	1.89			
24	4.5	2.10	6.40	1	1.96	7.00	1	3.41	5.18	3	3.09	6.67	-4.56	134	415
										3	3.60	3.12			
										4	4.29	1.87			

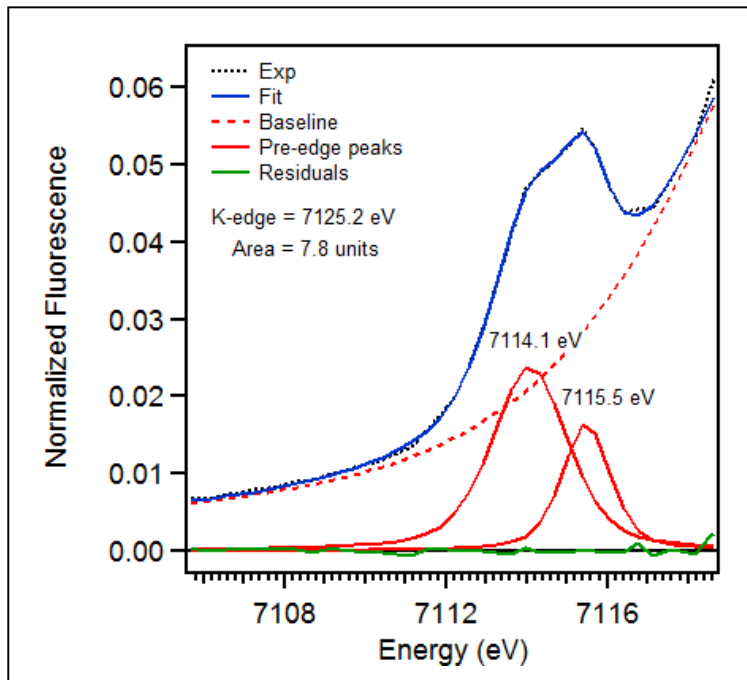


Figure S8. Pre-edge region analysis of hDOHH-D. The experimental data (black dotted), baseline (red dashed), pre-edge peak components (red solid), residuals (green solid) and total fit (blue solid) are shown.

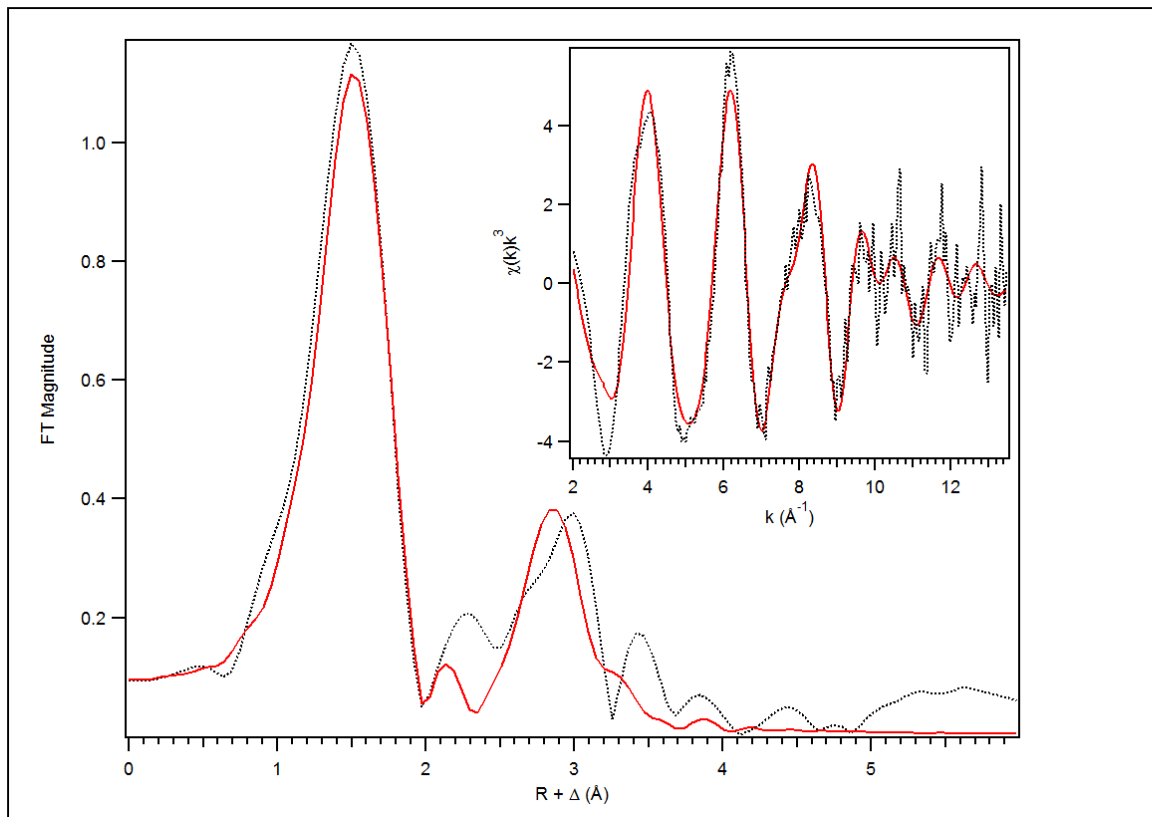


Figure S9. EXAFS spectrum of hDOHH-D. Fit A (red solid line) of the unfiltered (black dotted) EXAFS data (inset) and corresponding Fourier transform (Table S4, Fit 11). Fit A includes an Fe \cdots Fe distance at 3.07 Å. Data was fit between $k = 2 - 13.5 \text{ \AA}^{-1}$

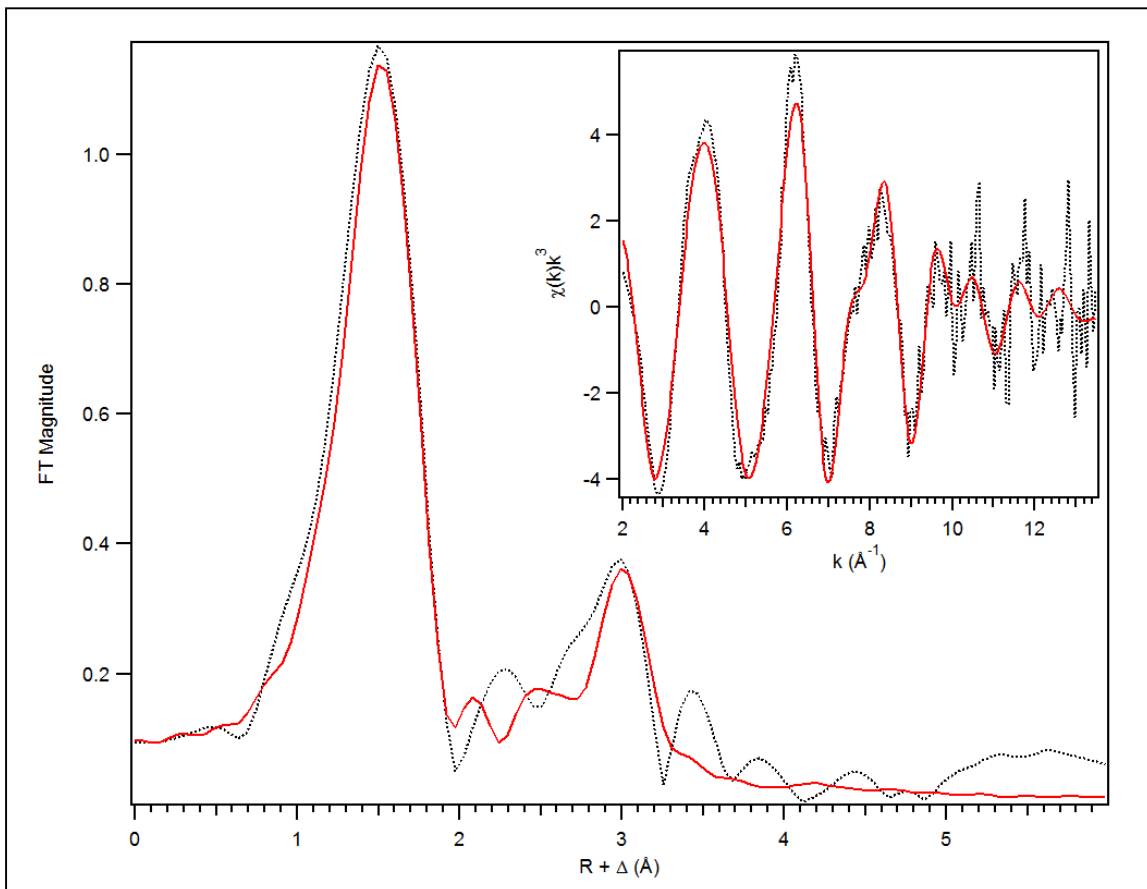


Figure S10. EXAFS spectrum of hDOHH-**D**. Fit B (red solid line) of the unfiltered (black dotted) EXAFS data (inset) and corresponding Fourier transform (Table S5, Fit 8). Fit B includes an Fe•••Fe distance at 3.42 Å and is the preferred fit for hDOHH-**D**. Data was fit between $k = 2 - 13.5 \text{ \AA}^{-1}$.

Table S4. Fit parameters for the unfiltered EXAFS data of hDOHH-**D** Fit A, between $k = 2 - 13.5 \text{ \AA}^{-1}$. Fit 11 gives the most reasonable fit of the experimental data.

	Fe-N				Fe-O				Fe•••Fe				Fe•••C				GOF		
Fit	N	R(Å)	$\sigma^2(10^{-3})$	E _o	F	F'													
1	6	2.03	8.25											-0.93	233	431			
2	5	2.03	6.92											-0.73	273	466			
3	4	2.03	5.57											-0.41	340	521			
4	5	2.07	5.50	1	1.93	0.87								-0.77	209	409			
5	5	2.08	6.35	2	1.94	3.93								-1.52	197	396			
6	4	2.09	4.43	2	1.96	2.78								-1.18	207	406			
7	3	2.10	2.32	2	1.95	1.74								-0.96	233	431			
8	4	2.09	4.58	2	1.95	2.88	1	3.07	6.22					-0.44	151	348			
9	4	2.10	4.56	2	1.96	2.68				4	3.09	4.46	0.42	178	377				
10	4	2.09	4.36	2	1.95	2.72				4	3.07	7.03	-0.39	127	319				
										4	3.43	2.27							
11	4	2.07	4.05	2	1.93	2.81	1	3.07	9.87	5	3.41	3.51	-2.90	133	326				

Table S5. Fit parameters for the unfiltered EXAFS data of hDOHH-**D** Fit B, between $k = 2 - 13.5 \text{ \AA}^{-1}$. Fit 8 gives the most reasonable fit of the experimental data.

	Fe-N				Fe-O				Fe $\cdots\cdots$ Fe				Fe $\cdots\cdots$ C				GOF		
Fit	N	R(Å)	$\sigma^2(10^{-3})$	N	R(Å)	$\sigma^2(10^{-3})$	N	R(Å)	$\sigma^2(10^{-3})$	N	R(Å)	$\sigma^2(10^{-3})$	E _o	F	F'				
1	6	2.03	8.23										-0.95	233	431				
2	5	2.03	6.91										-0.75	273	466				
3	4	2.03	5.56										-0.44	340	521				
4	4	2.07	3.60	1	1.93	-0.20							-0.41	237	435				
5	4	2.09	4.44	2	1.94	2.82							-1.22	206	405				
6	5	2.08	6.39	2	1.94	3.97							-1.49	197	396				
7	4	2.08	4.20	2	1.94	2.89	1	3.41	3.97				-1.97	141	336				
8	4	2.09	4.45	2	1.95	2.88	1	3.42	5.09	3	3.08	4.90	-0.69	127	317				
9	4	2.09	4.25	2	1.94	2.73				5	3.43	3.62	-1.28	125	316				
										3	3.09	4.73							
10	4	2.09	4.58	2	1.95	2.74				3	3.10	2.65	0.01	166	364				

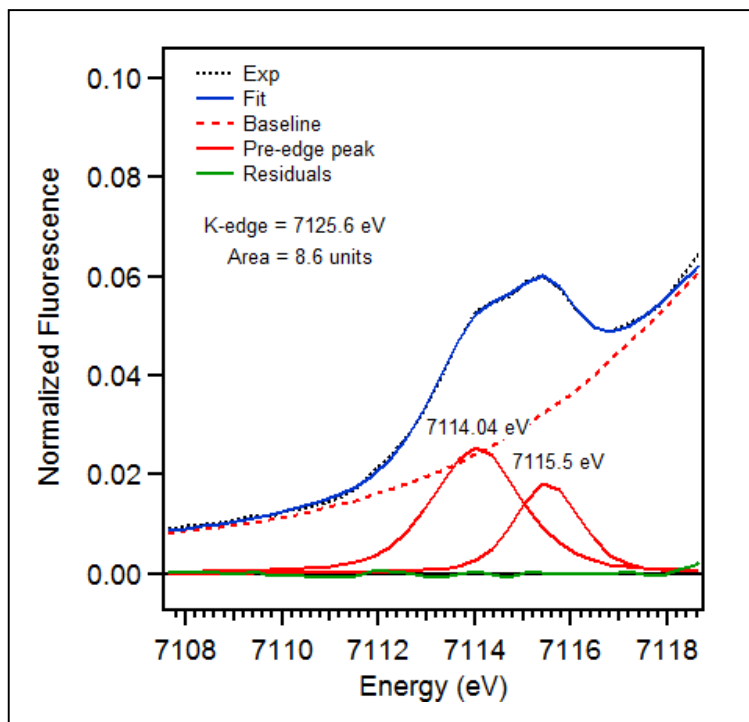


Figure S11. Pre-edge region analysis of hDOHH-**D** \bullet **S**. The experimental data (black dotted), baseline (red dashed), pre-edge peak components (red solid), residuals (green solid) and total fit (blue solid) are shown.

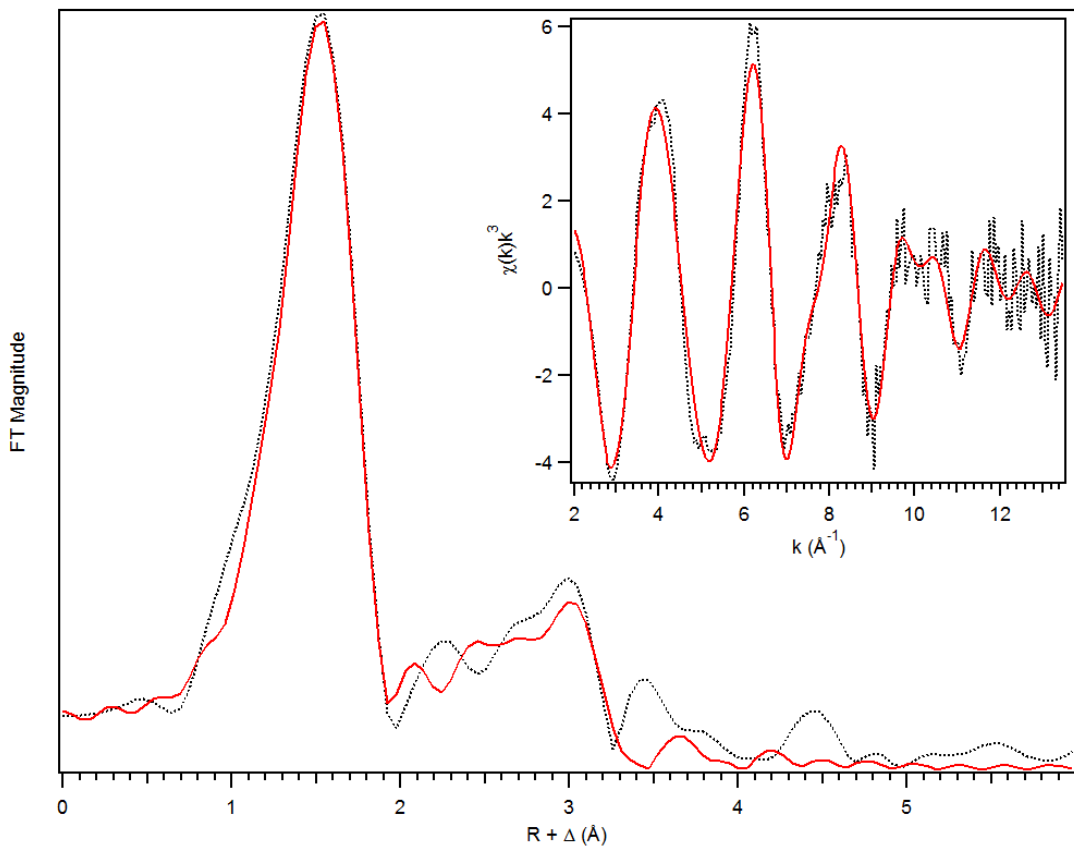


Figure 2. Fit (red solid line) of the unfiltered (black dotted) EXAFS data (inset) and corresponding Fourier transform (Fit 8, Table 1). $k = 2 - 13.5$, Fe @ 3.42 Å. hDOHH-**D•S**

Figure S12. EXAFS spectrum of hDOHH-**D•S**. Fit (red solid line) of the unfiltered (black dotted) EXAFS data (inset) and corresponding Fourier transform (Table S6, Fit 10). Data was fit between $k = 2 - 13.5$ Å⁻¹.

Table S6. Fit parameters for the unfiltered EXAFS data of hDOHH-**D•S**, between $k = 2 - 13.5 \text{ \AA}^{-1}$ ¹. Fit 10 gives the most reasonable fit of the experimental data.

Fit	Fe-N				Fe-O				Fe...Fe				Fe...C				GOF		
	N	R(Å)	$\sigma^2(10^{-3})$	E_o	F	F'													
1	6	2.03	7.49										-0.91	181	376				
2	5	2.03	6.21										-0.70	218	412				
3	4	2.03	4.89										-0.41	284	471				
4	3	2.03	3.46										-0.19	391	552				
5	5	2.06	5.29	1	1.93	0.95							-0.60	163	356				
6	5	2.07	6.59	2	1.94	4.34							-1.39	157	350				
7	4	2.08	4.44	2	1.95	2.78							-0.96	161	354				
8	4	2.07	4.20	2	1.94	2.79	1	3.42	4.96				-1.54	113	297				
9	4	2.08	4.20	2	1.95	2.56	1	3.44	6.17	3	3.08	5.33	-0.45	97	274				
10	4	2.08	4.40	2	1.95	2.88	1	3.42	3.51	3	3.08	6.29	-0.71	85	258				
										3	3.59	3.30							
11	4	2.08	4.23	2	1.90	2.56	1	3.44	6.14	3	3.08	5.49	-0.37	94	271				
										3	4.27	6.60							
12	4	2.08	4.51	2	1.95	2.96	1	3.42	3.30	3	3.08	6.43	-0.55	77	245				
										3	3.59	2.68							
										3	4.27	5.46							

Table S7. Component analysis of pre-edge peak fitting for hDOHH species. Pre-edge peaks were fit between 7108 – 7118 eV using PseudoVoigt functions with a 50:50 Gaussian/Lorentzian peak shape.

Species	Component Position (eV)	Component Area (units)	Total Area (units)
hDOHH- R	7110.4	1.93	8.6
	7111.9	6.20	
	7112.5	0.43	
hDOHH- P	7112.9	1.67	12.4
	7114.5	10.7	
hDOHH- P•S	7113.7	5.82	16.2
	7115.0	10.4	
hDOHH- D	7114.1	5.40	7.8
	7114.6	2.40	
hDOHH- D•S	7114.0	5.64	8.6
	7115.5	2.93	

Table S8. Selected distances from crystal structures of ferrous (Fe^{II}) synthetic model complexes.

Complex	Fe / Fe_2	Core OH _x	Fe-O (Å)	Term. OH _x	Fe-O (Å)	Fe \cdots Fe (Å)	$\angle\text{Fe-O-Fe}$	References
$[\text{Fe}_2(\mu\text{-OH})(\mu\text{-OH}_2)(\text{TPA})_2](\text{OTf})_2$	Fe_2	OH	2.098 2.034	-	-	3.216	95.5 °	¹
		OH_2	2.132 2.210	-	-	-	102.2 °	
$[\text{Fe}_2(\mu\text{-OH})_2(6\text{-Me}_3\text{-TPA})_2](\text{OTf})_2$	Fe_2	OH	2.033 2.208	-	-	3.221	98.8 °	²
$[\text{Fe}_2(\mu\text{-OH}_2)_2(\mu\text{-O}_2\text{CAr}^{4\text{F-Ph}})(\text{O}_2\text{CAr}^{4\text{F-}}_{\text{Ph}})_3(\text{THF})_2(\text{OH}_2)]$	Fe_2	OH_2	2.229 2.293 2.232 2.152	OH_2	2.115	3.288	93.3 ° 97.1 °	³
$[\text{Fe}_2(\mu\text{-OH}_2)_2(\mu\text{-O}_2\text{CAr}^{\text{Tol}})_2(\text{O}_2\text{CAr}^{\text{Tol}})_2(\text{THF})_2]$	Fe_2	OH_2	2.326 2.398	-	-	3.043	80.2 °	⁴
$[\text{Fe}_2(\mu\text{-OH})(\mu\text{-OAc})_2(\text{TACN})_2]\text{ClO}_4$	Fe_2	OH	1.987	-	-	3.317	113.1 °	⁵
$[\text{Fe}(\text{H}_2\text{O})_2(\overset{\text{Me}_2\text{BzIm}}{\text{Me}_2\text{BzIm}}\text{TACN})](\text{OTf})_2$	Fe	-	-	OH_2	2.113 2.148	-	-	⁶
$[\text{Fe}(\text{LN}_3\text{SMe})(\text{H}_2\text{O})_3](\text{OTf})_2$	Fe	-	-	OH_2	2.116 2.086 2.098	-	-	⁷
$[\text{Fe}(\text{indH})(\text{CH}_3\text{CN})(\text{H}_2\text{O})_2](\text{ClO}_4)_2$	Fe	-	-	OH_2	2.145 2.163	-	-	⁸
$[\text{Fe}(\text{H}_2\text{O})_6](\text{C}_{17}\text{H}_{13}\text{O}_7\text{S})_2 \bullet 8\text{H}_2\text{O}$	Fe	-	-	OH_2	2.138 2.155 2.043	-	-	⁹
$[\text{Fe}(\kappa\text{N-nicH})(\text{H}_2\text{O})_4]$	Fe	-	-	OH_2	2.135	-	-	¹⁰
$[\text{Fe}(\text{bpe})_4(\text{H}_2\text{O})_2](\text{TCNQ})_2$	Fe	-	-	OH_2	2.107 2.109	-	-	¹¹

TPA = tri-(2-pyridylmethyl)amine, 6-Me₃-TPA = tri-(6-methyl-2-pyridylmethyl)amine, O₂CAr^{4F-Ph} = 2,6-di-(p-tolyl)benzoate, TACN = N,N',N"-trimethyl-1,4,7-triazacyclononane,
 $\overset{\text{Me}_2\text{BzIm}}{\text{Me}_2\text{BzIm}}$ TACN = 1-(2-methyl-1-benzimidazolyl)methyl-4,7-dimethyl-1,4,7-triazacyclononane, indH = 1,3-bis(2'-pyridylimino)isoindoline, C₁₇H₁₃O₇S = bis(4',7-dimethoxyisoflavone-3'-sulfonate), nicH = pyridine-3-carboxylic acid, bpe = trans-1,2-bis(4-pyridyl)ethane, TCNQ = tetracyanoquinodimethane

Table S9. Selected distances from crystal structures of ferric (Fe^{III}) synthetic model complexes.

Complex	Fe / Fe_2	Core OH _x	Fe-O (Å)	Term. OH _x	Fe-O (Å)	Fe \cdots Fe (Å)	$\angle\text{Fe-O-Fe}$	References
$[\text{Fe}_2(\mu\text{-OH})_2(\text{H}_2\text{O})_2((\text{CH}_3)_2\text{NC}_7\text{H}_2\text{NO}_4)_2]$	Fe_2	OH	1.937 1.986	OH_2	2.033	3.118	105.3 °	¹²
$[\text{Fe}_2(\mu\text{-OH})(\mu\text{-OAc})_2(\text{HBpz}_3)_2]\text{ClO}_4$	Fe_2	OH	1.960 1.953	-	-	3.438	123.0 °	¹³
$[\text{Fe}_2(\mu\text{-OH})_2(\mu\text{-O}_2\text{C}\text{Ar}^{\text{Tol}})_2(\text{O}_2\text{C}\text{Ar}^{\text{Tol}})_2(4\text{-CNPy})_2]$	Fe_2	OH	1.978 1.945 1.997 1.945	-	-	2.831	92.4 °	¹⁴
$[\text{Fe}_2(\text{L}^{\text{amine}})_2(\mu\text{-OH})]\text{BPh}_4$	Fe_2	OH	2.003 2.017	-	-	3.762	138.6 °	¹⁵
$[\text{Fe}_2(\text{L}^{\text{NO}_2})_2(\mu\text{-OH})]\text{ClO}_4$	Fe_2	OH	1.969 2.003	-	-	3.733	140.1 °	¹⁶
$[\text{Fe}_2(\mu\text{-O})(\text{OH})(\text{OH}_2)(\text{TPA})_2](\text{ClO}_4)_3$	Fe_2	O	1.830 1.780	OH OH_2	1.914 2.041	3.389	138.9 °	¹⁷
$[\text{Fe}_2(\mu\text{-O})(\text{OH})(\text{OH}_2)(5\text{-Et-TPA})_2](\text{ClO}_4)_3$	Fe_2	O	1.826 1.779	OH OH_2	1.907 2.049	3.346	136.3 °	¹⁸
$[\text{Fe}(\text{tnpa})(\text{OH})(\text{PhCOO})]\text{ClO}_4$	Fe	-	-	OH	1.876	-	-	¹⁹
K[FeH ₃ 1(OH)]	Fe	-	-	OH	1.932 1.921	-	-	²⁰
$[\text{Fe}_2(\text{L}^{\text{Ph}^4\text{-O}})(\text{Ph}_3\text{CCO}_2)(\text{OH})](\text{ClO}_4)_2$	Fe_2	OR	2.051 2.008	OH	1.862	3.508	119.6 °	²¹
$[\text{Fe}(\text{OH})(\text{L}^1)][\text{K}(\text{DMF})_3]$	Fe	-	-	OH	1.857	-	-	²²
K[Fe 0^{Pr} (OH)]	Fe	-	-	OH	1.876	-	-	²³
$[\text{Fe}_2(\text{N-Et-HPTB})(\text{NO})(\text{OH})(\text{DMF})_2](\text{BF}_4)_3$	Fe_2	OR	1.952 2.044	OH	1.817 1.823	3.621	130.0 °	²⁴

$(\text{CH}_3)_2\text{NC}_7\text{H}_2\text{NO}_4$ = bis[4-dimethylamino-2,6-pyridinedicarboxylate], HBpz₃ = hydrotris(1-pyrazolyl)borate, O₂C Ar^{Tol} = 2,6-di-(p-tolyl)benzoate, 4-CNPy = 4-cyanopyridine, L^{amine} = 2,2'-(2-nethyl-2-(pyridin-2-yl)propane-1,3-diyl)bis(azanediyl)bis(methylene)diphenol, L^{NO₂} = 2,2'-(2-Methyl-2-(pyridine-2-yl)propane-1,3diyl)bis(azanediyl)-bis(methylene)bis(4-nitrophenol), TPA = tri-(2-pyridylmethyl)amine, 5-Et-TPA = 5-ethyl-tri-(2-pyridylmethyl)amine, tnpa = tris(6-neopentylamino-2-pyridylmethyl)amine), H₃1 = tris[(N'-tert-butylureaylato)-N-ethy]amine, L^{Ph⁴-O} = N,N,N',N'-tetrakis[(1-methyl-2-phenyl-4- imidazolyl)methyl]-1,3-diamino-2-propanolate), L¹ = tris(1-phenyl-2-(4-tert-butylalanine))amine, 0^{Pr} = Tris(N-isopropylcarbamoylmethyl)amine, N-Et-HPTB = N,N,N',N'- tetrakis[2-(1-ethylbenzimidazolyl)]-2-hydroxy-1,3-diaminopropane

Table S9 (continued). Selected distances from crystal structures of ferric (Fe^{III}) synthetic model complexes.

Complex	Fe / Fe_2	Core OH _x	Fe-O (Å)	Term. OH _x	Fe-O (Å)	Fe...Fe (Å)	<Fe-O-Fe	References
	Fe ₂	OR		OH				
$[\text{Fe}_2(\text{N-Et-HPTB})(\text{OH})_2(\text{DMF})_2](\text{BF}_4)_3$			1.979 2.044		1.817 1.823	3.954	129.1 °	²⁵
$[\text{Fe}_2(\mu\text{-OH})_2(\mu\text{-O}_2\text{CAr}^{\text{4F-Ph}})(\text{O}_2\text{CAr}^{\text{4F-Ph}})_3(\text{OH}_2)(2\text{-Ph}_2\text{P(O)-py})]$	Fe ₂	OH	1.981 1.955 1.977 1.981	OH ₂	2.099	2.973	98.2 ° 97.4 °	²⁶
$[\text{Fe}_2(\mu\text{-OH})(\text{OH}_2)_2(4\text{-Ph-hxta})]$	Fe ₂	OR	2.028 1.989	OH ₂	1.994	3.090	104.4 °	²⁷
		OH	1.956				100.6 °	
$[\text{Fe}_2(\mu\text{-OH})_2(\text{OH}_2)_2(\text{Dipic})_2]$	Fe ₂	OH	1.937 1.993	OH ₂	2.021	3.089	103.6 °	²⁸
$[\text{Fe}_2(\mu\text{-OH})_2(\mu\text{-O}_2\text{CAr}^{\text{Tol}})(\text{O}_2\text{CAr}^{\text{Tol}})_3(\text{OH}_2)(\text{Hdmpz})_2]$	Fe ₂	OH	1.945 1.958 2.013 1.953	OH ₂	2.013	2.996	100.3 °	²⁹
$[\text{Fe}_2(\mu\text{-O}_2)(\text{Ph}_3\text{PO})_2(\text{N-Et-HPTB})](\text{BF}_4)_3$	Fe ₂	OR OO	1.991 1.881	-	-	3.463	120.8 °	³⁰
$[\text{Fe}_2(\mu\text{-O}_2)(\mu\text{-O}_2\text{CPh})(\text{Ph-bimp})](\text{BF}_4)_2$	Fe ₂	OR	2.018 2.001	-	-	3.327	111.7 °	³¹
		OO	1.944 1.864					
$[\text{Fe}_2(\mu\text{-O}_2)(\mu\text{-O}_2\text{CCH}_2\text{Ph})_2\{\text{HB(pz')}_3\}]$	Fe ₂	OO	1.881 1.877	-	-	4.007	-	³²
$[\text{Fe}_2(6\text{Me}_2\text{-BPP})_2(\mu\text{-OH})(\mu\text{-O}_2)](\text{OTf})$	Fe ₂	OH	1.943 2.006	-	-	3.395	118.6 °	³³
		OO	1.887 1.867					

N-Et-HPTB = N,N,N',N'- tetrakis[2-(1-ethylbenzimidazolyl)]-2-hydroxy-1,3-diaminopropane, $\text{O}_2\text{CAr}^{\text{4F-Ph}} = 2,6\text{-di-(p-tolyl)benzoate}$, 2- $\text{Ph}_2\text{P(O)-py} = 2\text{-Pyridyldiphenylphosphine oxide}$, 4- $\text{Ph-hxta} = 2\text{- hydroxy-5-phenyl-1,3-xylylenedimethanamine-N,N,N',N'-tetraacetate}$, Dipic = 2,6-pyridinedicarboxylate, $\text{O}_2\text{CAr}^{\text{Tol}} = 2,6\text{-di-(p-tolyl)benzoate}$, Hdmpz = 3,5-dimethylpyrazole, Ph-bimp = 2,6-bis{bis{2-(1-methyl- 4,5-diphenylimidazolyl)methyl}aminomethyl}-4-methylphenolate, pz' = 3,5-bis(isopropyl)- pyrazole, 6Me₂-BPP = N,N-bis(6-methyl-2-pyridylmethyl-3-amino-propionic acid

References

- (1) Korendovych, I. V.; Kryatov, S. V.; Reiff, W. M.; Rybak-Akimova, E. V. *Inorg. Chem.* **2005**, *44* (24), 8656–8658.
- (2) Kryatov, S. V.; Taktak, S.; Korendovych, I. V.; Rybak-Akimova, E. V.; Kaizer, J.; Torelli, S.; Shan, X.; Mandal, S.; MacMurdo, V. L.; Mairata i Payeras, A.; Que, L. *Inorg. Chem.* **2005**, *44* (1), 85–99.
- (3) Yoon, S.; Lippard, S. J. *J. Am. Chem. Soc.* **2004**, *126* (51), 16692–16693.
- (4) Yoon, S.; Kelly, A. E.; Lippard, S. J. *Polyhedron* **2004**, *23* (17), 2805–2812.
- (5) Chaudhury, P.; Wieghardt, K.; Nuber, B.; Weiss, J. *Angew. Chem. Int. Ed. Engl.* **1985**, *24* (9), 778–779.
- (6) Mitra, M.; Lloret-Fillol, J.; Haukka, M.; Costas, M.; Nordlander, E. *Chem. Commun.* **2014**, *50* (12), 1408–1410.
- (7) Widger, L. R.; Siegler, M. A.; Goldberg, D. P. *Polyhedron* **2013**, *58*, 179–189.
- (8) Pap, J. S.; Cranswick, M. A.; Balogh-Hergovich, E.; Baráth, G.; Giorgi, M.; Rohde, G. T.; Kaizer, J.; Speier, G.; Que, L. *Eur. J. Inorg. Chem.* **2013**, No. 22-23, 3858–3866.
- (9) Zhang, Z.-T.; Cheng, X.-L. *Acta Crystallogr. C* **2005**, *61* (Pt 12), m529–m531.
- (10) Liang, Y.; Li, W.; Guo, B.-J. *Acta Crystallogr. Sect. E Struct. Reports Online* **2005**, *61* (9), m1782–m1784.
- (11) Galet, A.; Muñoz, M. C.; Agustí, G.; Martínez, V.; Gaspar, A. B.; Real, J. A. *Z. Anorg. Allg. Chem.* **2005**, *631* (11), 2092–2095.
- (12) Ou, C.-C.; Lalancette, R. A.; Potenza, J. A.; Schugar, H. J. *J. Am. Chem. Soc.* **1978**, *100* (7), 2053–2057.
- (13) Turowski, P. N.; Armstrong, W. H.; Liu, S.; Brown, S. N.; Lippard, S. J. *Inorg. Chem.* **1994**, *33* (4), 636–645.
- (14) Yoon, S.; Lippard, S. J. *J. Am. Chem. Soc.* **2005**, *127* (23), 8386–8397.
- (15) Shakya, R.; Powell, D. R.; Houser, R. P. *Eur. J. Inorg. Chem.* **2009**, *2009* (35), 5319–5327.
- (16) Jozwiuk, A.; Ingram, A. L.; Powell, D. R.; Moubaraki, B.; Chilton, N. F.; Murray, K. S.; Houser, R. P. *Dalton Trans.* **2014**, *43* (25), 9740–9753.
- (17) Hazell, A.; Jensen, K. B.; McKenzie, C. J.; Toftlund, H. *Inorg. Chem.* **1994**, *33* (14), 3127–3134.
- (18) Dong, Y.; Fujii, H.; Hendrich, M. P.; Leising, R. A.; Pan, G.; Randall, C. R.; Wilkinson, E. C.; Zang, Y.; Que, L. *J. Am. Chem. Soc.* **1995**, *117* (10), 2778–2792.

- (19) Ogo, S.; Wada, S.; Watanabe, Y.; Iwase, M.; Wada, A.; Harata, M.; Jitsukawa, K.; Masuda, H.; Einaga, H. *Angew. Chem. Int. Ed. Engl.* **1998**, *37* (15), 2102–2104.
- (20) MacBeth, C. E.; Gupta, R.; Mitchell-Koch, K. R.; Young, V. G.; Lushington, G. H.; Thompson, W. H.; Hendrich, M. P.; Borovik, A. S. *J. Am. Chem. Soc.* **2004**, *126* (8), 2556–2567.
- (21) Yamashita, M.; Furutachi, H.; Toshia, T.; Fujinami, S.; Saito, W.; Maeda, Y.; Takahashi, K.; Tanaka, K.; Kitagawa, T.; Suzuki, M. *J. Am. Chem. Soc.* **2007**, *129* (1), 2–3.
- (22) Celenligil-Cetin, R.; Paraskevopoulou, P.; Dinda, R.; Staples, R. J.; Sinn, E.; Rath, N. P.; Stavropoulos, P. *Inorg. Chem.* **2008**, *47* (3), 1165–1172.
- (23) Mukherjee, J.; Lucas, R. L.; Zart, M. K.; Powell, D. R.; Day, V. W.; Borovik, A. S. *Inorg. Chem.* **2008**, *47* (13), 5780–5786.
- (24) Majumdar, A.; Lippard, S. J. *Inorg. Chem.* **2013**, *52* (23), 13292–13294.
- (25) Majumdar, A.; Apfel, U.-P.; Jiang, Y.; Moënne-Loccoz, P.; Lippard, S. J. *Inorg. Chem.* **2014**, *53* (1), 167–181.
- (26) Carson, E. C.; Lippard, S. J. *Inorg. Chem.* **2006**, *45* (2), 837–848.
- (27) Schmitt, W.; Murugesu, M.; Goodwin, J. C.; Hill, J. P.; Mandel, A.; Bhalla, R.; Anson, C. E.; Heath, S. L.; Powell, A. K. *Polyhedron* **2001**, *20* (11-14), 1687–1697.
- (28) Thich, J. A.; Ou, C. C.; Powers, D.; Vasiliou, B.; Mastropaoletti, D.; Potenza, J. A.; Schugar, H. J. *J. Am. Chem. Soc.* **1976**, *98* (6), 1425–1433.
- (29) Yoon, S.; Lippard, S. J. *J. Am. Chem. Soc.* **2004**, *126* (9), 2666–2667.
- (30) Dong, Y.; Yan, S.; Young, V. G.; Que, L. *Angew. Chem. Int. Ed. Engl.* **1996**, *35* (6), 618–620.
- (31) Ookubo, T.; Sugimoto, H.; Nagayama, T.; Masuda, H.; Sato, T.; Tanaka, K.; Maeda, Y.; Ōkawa, H.; Hayashi, Y.; Uehara, A.; Suzuki, M. *J. Am. Chem. Soc.* **1996**, *118* (3), 701–702.
- (32) Kim, K.; Lippard, S. J. *J. Am. Chem. Soc.* **1996**, *118* (20), 4914–4915.
- (33) Zhang, X.; Furutachi, H.; Fujinami, S.; Nagatomo, S.; Maeda, Y.; Watanabe, Y.; Kitagawa, T.; Suzuki, M. *J. Am. Chem. Soc.* **2005**, *127* (3), 826–827.